



Comprehensive Phytochemical Profiling, GC-MS Analysis, Molecular Docking and Antiproliferative Activity of Ethanol Fraction of *Tabernaemontana coronaria* and *Thunbergia alata*

Swapna Neela^{1,2*}, Makula Ajitha³ and Vijaya Kuchana⁴

¹Jawaharlal Nehru Technological University, Kukatpally, Hyderabad - 500085, Telangana, India; swapnaneela1982@gmail.com

²Department of Pharmaceutics, Nalla Narasimha Reddy Education Society's Group of Institutions, School of Pharmacy, Ghatkesar, Hyderabad - 500088, Telangana, India

³Department of Pharmaceutical Chemistry, JNTUH College of Pharmacy, Sultanpur, Sangareddy - 502273, Telangana, India

⁴Department of Pharmaceutical Chemistry, Teegala Krishna Reddy College of Pharmacy, Meerpet, Hyderabad - 500097, Telangana, India

Abstract

Objective: Current study involves the phytochemical examination, GC MS testing of ethanol fraction of leaves of two plants *Tabernaemontana coronaria* and *Thunbergia alata*. **Methods:** Both ethanol fractions of selected plants were subjected to *In vitro* antiproliferative activity by employing MTT assay on A549 cell lines. Zebra Fish fin model and zebra fish embryo tests were employed to assess the fin regeneration and effect on angiogenesis respectively. **Results:** The phytochemical screening discovered existence of terpenoids, proteins, carbohydrates, phenols, tannins, saponins, flavonoids, glycosides, and alkaloids in both *T. coronaria* and *T. alata*. The GC MS profile of the ethanol portion of *T. coronaria* leaves identified 16 components, while the ethanol fraction of *T. alata* leaves had 14 components. The molecular docking experiments showed that compound 1 and compound 4 had favorable docking energies of $-8.7 \text{ kcal.mol}^{-1}$ and $-8.2 \text{ kcal.mol}^{-1}$, correspondingly, in the site of JNK-1 kinase. Compound 4 established hydrogen bond interactions with Ser34 and Asp169 in the catalytic and DFG motif regions of the JNK-1, respectively. Compounds 3 and 7, with docking energies of -6.4 and $-7.9 \text{ kcal.mol}^{-1}$, correspondingly, also resided in active motif of JNK-1. Compound 2 had docking energy of $-5.4 \text{ kcal.mol}^{-1}$ and was well placed in the protein cavity. Regarding the binding of compounds in the KAS III, compound 4 had an excellent docking energy of $-8.0 \text{ kcal.mol}^{-1}$, and compound 2 had docking energy $-5.9 \text{ kcal.mol}^{-1}$. Both compounds were well placed in the active pocket of KAS III macromolecule and established hydrogen bond interactions with Asn260 and Arg262. Compound 4 also established hydrophobic contacts with Arg46 and Arg223. **Conclusion:** The study states that *T. coronaria* and *T. alata* treatment strongly inhibited A549 cells viability, and cell volume expansion, which result in cell proliferation. Likewise, a noteworthy decrease in fin regeneration and reduction in percentage vessel growth was observed in zebra fish and embryo assays.

Keywords: Angiogenesis, Bioactive Compounds, Docking, Phytochemicals, Zebra Fish

1. Introduction

Due to bioactive compounds, plants have long served as resource of numerous powerful medicines for

pharmaceutical business¹. Phytochemicals possess individual, additive, or synergistic activities and are valuable in treating various ailments, contributing to improved health outcomes^{2,3}. The role of

*Author for correspondence

phytochemicals is essential in the pharmaceutical sector for developing new medicines and design of therapeutics⁴. Discovering active principles in natural resources is first place in developing novel drugs. Testing extracts is an inventive method for identifying medicinally valuable compounds in various plant species⁵. Phytochemicals include terpenoids, alkaloids, saponins, tannins, and flavonoids that exhibit various pharmacological properties, including anticancer, anti-ulcer, anti-diarrheal, anti-inflammatory, antioxidant activities, and among others.

Tabernaemontana coronaria, member of Apocynaceae family unit, is a persistent shrub with a potential spread of up to three meters. The leaves of this plant are elongated and exhibit wavy margins, with a glossy yet dull green appearance. It is an ornamental plant rich in numerous alkaloids and other phytochemical constituents such as phenolic compounds, glycosides, steroids, and terpenoids. In traditional medicine, *T. coronaria* has been employed to cure for a range of ailments such as scorpion and wind envenomation, sore eyes, gastric disorders, inflammation, skin diseases, cancer, and hypertension⁶⁻⁹.

Thunbergia alata, a perennial vine belonging to the Acanthaceae family, can grow up to five meters long and is commonly propagated via seeds. The flowers of this species are yellow to orange and bloom continuously throughout the year. The fruit is a depressed globular capsule that bears four seeds and is produced year-round. The herb is predominantly scattered in the western and eastern ghats. The herb holds significant value in traditional medicine for treating inflammations, fevers, dysentery, cough, pains, skin infections, and other maladies. Phytochemical study of herb had investigated occurrence of polyphenolic compound and glycosides¹⁰⁻¹³. Due to the pharmacological applications of *T. coronaria* and *T. alata*, the aimed to analyze the phytoconstituents that are involved in such activities.

Cancer continues to be a leading cause of mortality on a global scale^{14,15}. As such, there is an immediate need to develop novel therapeutic approaches for this disease, particularly given that current treatment strategies rely heavily on radiation-based therapy and chemotherapy¹⁶, both associated with significant toxicities¹⁷. As a result, alternative and integrative medicines have gained popularity as optimistic methods for treating cancer¹⁸. This study endeavors

to assess the potential anti-proliferative potential of natural products, the results of which have thus far been exceedingly promising¹⁶.

An effective analytical technique enabling the quantification and identification of phytochemicals in plants is gas chromatography-mass spectrometry (GC-MS)¹⁹. GC-MS testing is essential for chemotaxonomic classification and phytochemical characterization of medicinal flora that contain physiologically active component²⁰. Computational chemistry has provided researchers with novel tools to investigate the interactions between receptor protein residues and ligands. Docking practice is a powerful tool to understand the contact of a putative site by a given ligand and to facilitate drug invention^{21,22}. In this investigation, we intended to conduct phytochemical profiling and assess antiproliferative potential of the ethanol fraction derived from *T. coronaria* and *T. alata*.

2. Materials and Methods

2.1 Plant Material

T. alata and *T. coronaria* vegetation was gathered through the countryside of Tirupati and Chittoor and legitimated by Dr. K. Venkata Ratnam (assistant professor) from botany section at Rayalaseema University (Kurnool, AP, India). For future reference, voucher specimens (RU/BD/VSN-142 and 163) have been submitted.

2.2 Extracts Preparation

Leaves of *T. alata* and *T. coronaria* got collected and dried in the shadow. Dry leaves then got powdered and extracted thoroughly with ethanol by soxhlet apparatus. Solvent was evaporated at room temperature by keeping the extract open to the atmosphere to get dry solid extract, and the % yield got determined²³.

2.3 Phytochemical Screening

Standard procedures were used to conduct a preliminary phytochemical analysis of leaf extracts from *T. coronaria* and *T. alata* in ethanol and petroleum ether. The EETA (Ethanol Extract of *T. alata*) and EETC (Ethanol Extract of *T. coronaria*) were examined for existence of several phytoconstituents like triterpenoids, tannins, saponins, polyphenolic components, flavonoids, and carbohydrates^{24,25}.

2.4 GC-MS Testing

This testing was conducted using 7890A gas chromatograph (GCMSQP2010, SHIMADZU) with a mass spectrophotometer. System got equipped by HP-5 MS merged silica column (phenyl methyl siloxane, 30.0m×250µm, 0.25µm-thickness) connected to 5675C MSD by triple-axis screener. Helium got applied with a flow rate of 1.0 ml per min. The GC-MS conditions included a 1 µl injector in split form by a split proportion of 1:50 and injection point of 300°C, and an ion supply temperature 250°C, crossing point of 300°C, pressure 16.2 psi, and time 1.8 mm. Column started at 36°C (5 min) and was gradually adjusted to 150°C at pace of 4°C per min. Temperature increased to 250°C at pace of 20°C per min and maintained to 5 min. Elution time found as 37 min. Percent sum of every constituent got determined by evaluating its mean peak region to the whole area. The MS-Solution software was used to manage system and collect data^{26,27}.

2.5 Identification of Compounds

The National Institute of Standards and Technology (NIST) database was utilized to identify components by interpreting their retention values and mass spectrum. More than 62,000 patterns of well-known substances are included in the database. The acquired spectra of the unknown *T. coronaria* and *T. alata* fractions were compared with the reference mass spectra of the identified components kept in the NIST library (NISTII).

2.6 Molecular Docking

2.6.1 Information Regarding JNK-1 Crystal Structure and its Active Site Topology with Docking Details

Janus kinase-1 (JNK-1) is a type of receptor tyrosine kinases which is crucial for the cancer cell development differentiation and proliferation. The crystal structure PDB ID: 3V3V complexed with a natural molecule quercetin was employed for molecular docking. The general architecture of JNK-1 is similar to other receptor tyrosine kinases (RTYK's) that constitutes of N-terminal (Asp7-Met108) and C-terminal (Val186-Ala332) lobes, a short motif that connects the two terminals i.e. a hinge region (Glu109-Met121) and is further extended as activation loop that consists of

two main motifs namely DFG (Asp169, Phe170 and Gly171) and HRD (His149, Arg150 and Asp151).

An active site of EGFR protein is formed with a gap amid N and C-terminals with a hinge region is known as ATP binding site to which an ATP binds. The active site contains a catalytic, hinge and DFG motif that is selective for the inhibitor binding which states the type of inhibitor according to the binding fashion. The Quercetin i.e. the co-crystallized ligand developed contacts with Glu109, Met111 and Asn114 in the hinge region, Lys54 in the catalytic region, Asp169 in the DFG motif and Glu173 in the side chain region as shown in Figure 1. Further to validate the docking protocol the co-crystallized ligand was redocked as shown in Figure 2^{28,29}.

2.7 Antiproliferative Activities

2.7.1 Morphological Screening

2.7.1.1 Cell culture

Human lung adenocarcinoma (A549) cancer cell lines were subculture on site for the investigation. The ATCC is the cell line's original source. Cells got cultivated in 75cm² Corning bottle canted necked vented flasks by DMEM and kept at 37°C in humidifying 5% CO₂ setting. Cells got cultured in DMEM (gibco *in vitro* gen, Paisley, UK) with 1% amphotericin (250 U/mL), 1% streptomycin (1000 µg/mL), 1% penicillin (1000U/mL), 1% non-essential amino acids and 10% FES as supplements for passages 30 to 50. The cells were subcultured in 75cm² plastic flasks at density of 2.2x10⁴ cells/cm² after being enzymatically passaged using 0.25% trypsin-1mM EDTA. Every 2 days, the culture medium was replaced. Microscopic observation indicated that 80% of the cells were confluent.

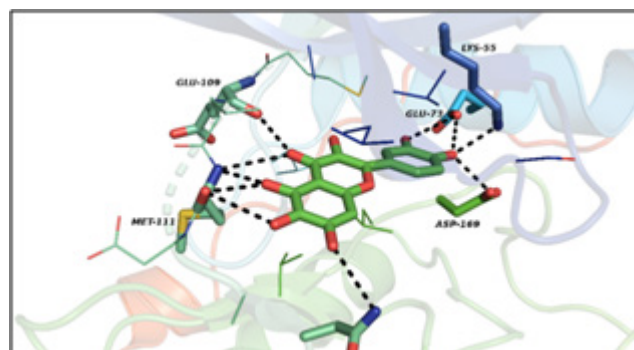


Figure 1. Quercetin in complexed with JNK-1.

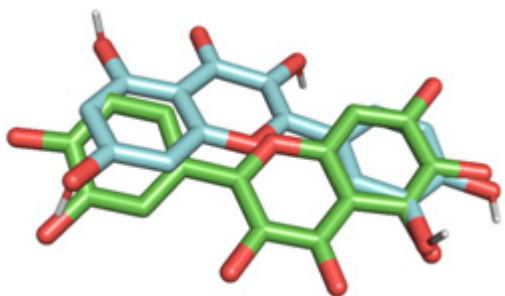


Figure 2. Alignment of co-crystallized ligand (green) and re-docked co-crystallized ligand (grey).

2.7.1.2 Procedure

A-549 cells were treated with test plant extracts (50 μg) and 25 μg of the standard drug. Following treatment with test compounds, cells were monitored for 24, 48, and 72 hours. axiovert 200M phase microscope at a 10x magnification was in use to capture the images. The pictures were taken with axiovision Rel.4.2 software^{30,31}.

2.7.2 Zebra Fish Caudal Fin Test

Fin regeneration was primarily been considered post amputating the tail fin portion through a simple removal method. Re-epithelialization takes place in the wound a few hours after the fin is amputated. Zebrafish were anesthetized with 0.04% MS-222 (tricaine) prior to and during the caudal fin amputation procedures. A razor blade was employed to amputate the caudal fin of the fish perpendicular to its cranio-caudal axis (around 50% lesion size).

Five groups of zebrafish were housed in tanks under controlled setting with 14-hour light/10-hour dark cycle and a temperature of 28 ± 0.5 °C. Prior to amputation, the fish were anesthetized with 0.04% MS-222 for a few minutes until the gills ceased movement. The caudal fins were then amputated at the mid-fin level while the fish were placed on glass slides. Following amputation, the fish were promptly transferred to a recovery tank and recovered within three minutes. Bevacizumab (25 μg /150 ml) and test extracts were administered to various tanks for 7 days post-amputation (dpa) at 28 ± 0.5 °C, and measurements of the length of regenerating blood vessels and fins were recorded from images. With six fins per group, the experiment was conducted three times independently.

2.7.3 Zebra Fish Embryo Model Assay

Zebra fish got kept in glass tanks at 28°C and subjected to 14-hour light/10-hour dark set. Fish of both sexes were maintained in separate tanks with a constant oxygen supply at a 2:1 ratio. The fish were not fed for three days before being provided with food for seven consecutive days. The male and female are maintained together in one tank on the eleventh day. One day after mating, fish are kept in their own tanks, and embryos are harvested using an embryo collector with a mesh size of 0.9 mm.

In 10L of fish system water, 10g of methylene blue, 0.81g of magnesium sulfate, 0.49g of calcium chloride, 0.13g of potassium chloride, and 2.94g of sodium chloride were dissolved to make the embryo media. Embryos were washed in embryo media before being placed in a beaker. Each well of a microtiter plate is filled with 100 ml of embryo media that contains a blank, a test substance (10, 20, and 40 μg /100 ml), and a reference drug. One embryo was introduced to each well on the microtiter plate using a dropper.

The embryos were kept after treatment with drug in each well of culture plate at 28.5°C for 72 hrs post fertilization (hpf). Embryos were visually examined with a frequency of 24 hrs for 3 days (24hrs, 48hrs, and 72hrs) for neovascularization and other phenotypic alterations such as pericardial edema, stunted development, delayed hatching, haemorrhages, abdominal extension of the yolk sac, and tail bending by a trinocular microscope through blue filters, and images got taken using a digital camera. This was done after 24, 48, and 72 hpf of drug addition to the wells.

2.8 Statistical Analysis

Average \pm SEM (n=6) used to articulate experimental results. One-way ANOVA analyzed results. The findings of p value < 0.005 deemed significant.

3. Results and Discussion

3.1 Phytochemical Testing

Phytochemical testing of ethanol fraction of *T. coronaria* and *T. alata* leaves have incidence of terpenoids, proteins, carbohydrates, phenols, tannins, saponins, flavonoids, glycosides, and alkaloids as shown in Table 1.

3.2 GC-MS Profile of Ethanol Extract of *T. coronaria* Leaf

16 components were noticed from the GC-MS investigation of ethanol division of *T. coronaria* takes off showing different phytochemical exercises. Table 2 presents the chemical constituents found in the EETC along with their corresponding Area (%), Molecular weight (MW), atomic equation, and Retention Time (RT).

Table 1. Phytochemical testing of *T. coronaria* and *T. alata*

Phytochemicals	<i>Tabernaemontana coronaria</i> Ethanol extraction	<i>Thunbergia alata</i> . Ethanol extraction
Saponins	+	+
Amino acids	+	-
Carbohydrates	+	+
Proteins	+	-
Tannins	+	+
Steroids	-	+
Terpenoids	+	+
Flavonoids	+	+
Glycosides	+	+
Alkaloids	+	+

- indicates the absence and + indicates the presence of phytochemicals

3.3 GC-MS Profile of Ethanol Extract of *T. alata* Leaf

14 components were distinguished from the GC-MS investigation of ethanol division of *T. alata*, showing different phytochemical exercises. Table 3 presents the chemical constituents within the EETA along with their corresponding area (%), Molecular Weight (MW), atomic equation, and Retention Time (RT).

3.4 Molecular Docking

3.4.1 Docking of Selected Compounds of *T. coronaria* against JNK-1 Kinase

Compound 1 with an encouraging docking energy $-8.7 \text{ kcal.mol}^{-1}$ occupied active location of JNK-1 kinase; oxygen of triazinone moiety interacted via two hydrogen bonds with Glu109 and Met111 in the hinge region further the oxygen and nitrogen of the nitro functionality developed four hydrogen bond interactions with Asp169, Lys55 and Glu73 in the DFG, catalytic and side chain region of the pocket. The phenyl ring attached on the 4th position of the triazinone core established π -sigma and π - π and π -alkyl electrostatic and hydrophobic interactions with Ile32, Val40, Ala53, Val158 and Leu168 as shown in Figure 3A.

Compound 4 resided in the active pocket of JNK-1 macromolecule establishing hydrogen bond

Table 2. Chemical components in ethanol fraction: *T. coronaria* leaves

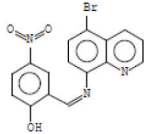
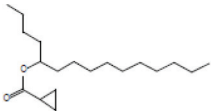
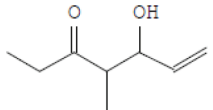
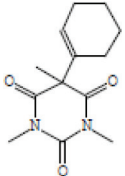
S. No.	RT	Area%	Components name	M.F	M.W g per mol	Structure
1	0.100	4.70	5-Bromo-8-(5-nitrosalicylideneamino)quinoline hydrochloride	$\text{C}_{16}\text{H}_{10}\text{BrN}_3\text{O}_3$	371	
2	0.035	5.72	5-Cyclopropylcarbonyl oxypentadecane	$\text{C}_{19}\text{H}_{36}\text{O}_2$	296	
3	1.384	0.43	6-Hepten-3-one, 5-hydroxy-4-methyl-	$\text{C}_8\text{H}_{14}\text{O}_2$	142	
4	0.415		2,4,6 (1H, 3H, 5H)-Pyrimidinetrione, 5-(1-cyclohexen-1-yl)-1,3,5-trimethyl-	$\text{C}_{13}\text{H}_{18}\text{N}_2\text{O}_3$	250	

Table 2. Continued...

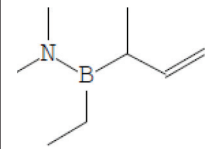
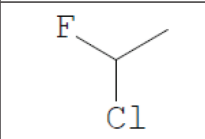
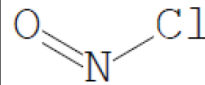
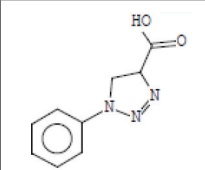
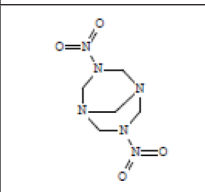
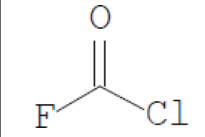
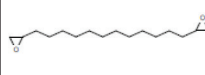
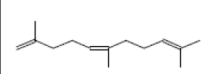
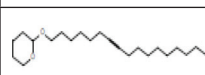
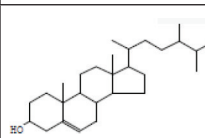
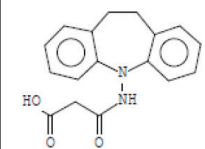
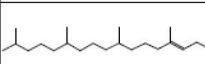
S. No.	RT	Area%	Components name	M.F	M.W g per mol	Structure
5	1.651	0.06	Boranamine, 1-ethyl-N,N-dimethyl-1-(1-methyl-2-propenyl)-	C ₈ H ₁₈ BN	139	
6	1.490	0.26	Ethane, 1-chloro-1-fluoro-	C ₂ H ₄ ClF	82	
7	4.180	0.59	Nitrosyl chloride	ClNO	65	
8	2.458	9.60	1H-1,2,3-Triazole-4-carboxylic acid, 4,5-dihydro-1-phenyl	C ₉ H ₉ N ₃ O ₂	191	
9	4.980	0.41	N,N-Dinitro-1,3,5,7-tetrazabicyclo[3,3,1]nonane	C ₅ H ₁₀ N ₆ O ₄	218	
10	4.346	-0.10	Carbonic chloride fluorid	CClFO	82	
11	22.84	0.113	1,2-15,16-Diepoxyhexadecane	C ₁₆ H ₃₀ O ₂	254	
12	28.734	0.35	1,5,9-Undecatriene, 2,6,10-trimethyl-, (Z)-	C ₁₄ H ₂₄	192	
13	31.65	0.35	2H-Pyran, 2-(7-heptadecyloxy) tetrahydro-	C ₂₂ H ₄₀ O ₂	336	
14	32.08	1.48	5-Cholestene-3-ol, 24-methyl-	C ₂₈ H ₄₈ O	400	
15	36.151	0.20	N-(10,11-Dihydro-5H-dibenzo[b,f]azepin-5-yl)malonic acid	C ₁₇ H ₁₆ N ₂ O ₃	296	
16	34.13	0.60	3,7,11,15-Tetra methyl-2-hexadecen-1-ol	C ₂₀ H ₄₀ O	296	

Table 3. Chemical components in ethanol fraction: *T. alata* leaves

S. No.	RT	Area%	Component name	M.F.	M.W g per mol	Structure
1	0.066	12.04	2-Chloro-3-hydroxy-butyric acid	C ₄ H ₇ ClO ₃	138	
2	0.260	2.43	N-[3,4-Dimethoxyphenyl]-p-toluenesulfonamide	C ₁₅ H ₁₇ NO ₄ S	307	
3	0.690	1.63	5-Bromo-8-(5-nitrosalicylideneamino) quinoline hydrochloride	C ₁₆ H ₁₀ BRN ₃ O ₃	371	
4	0.840	0.29	Propanimidamide, N-(1-chloro-1-propenyl)-, monohydrochloride	C ₆ H ₁₂ C ₁₂ N ₂	182	
	0.760	0.42	4-(4-Nitroanilino)-6-piperidino-1,2,3-triazin-2(1H)-one hydrochloride	C ₁₄ H ₁₆ N ₆ O ₃	316	
6	1.290	0.07	Ethane, 1-chloro-1-fluoro-	C ₂ H ₄ ClF	82	
7	0.975	0.50	1-Hexanamine, 6,N-dihydroxy-	C ₅ H ₁₃ NO ₂	119	
8	1.158	5.27	Silanamine, N-phenyl-	C ₆ H ₉ NSi	123	
9	5.215	0.79	N,N-Dinitro-1,3,5,7-tetrazabicyclo[3,3,1]nonane	C ₅ H ₁₀ N ₆ O ₄	218	
10	2.325	0.51	Propanoic acid, 2-oxo-, ethyl ester	C ₅ H ₈ O ₃	116	
11	2.404	0.22	2-Propanone, 1,1-dichloro-	C ₃ H ₄ C ₁₂ O	126	
12	32.116	0.16	Benz[e]azulene-3,8-dione, 5-[(acetyloxy)methyl]-3a,4,6a,7,9,10,10a,10b-octahydro-3a,10a-di	C ₁₉ H ₂ O ₆	348	

Table 3. Continued...

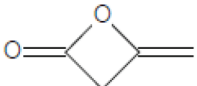
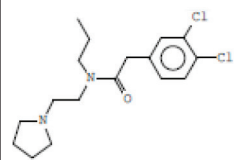
S. No.	RT	Area%	Component name	M.F.	M.W g per mol	Structure
13	5.628	0.52	2-Oxetanone, 4-methylene-	C ₄ H ₄ O ₂	84	
14	6.039	0.33	3-Azahexane, N-[3,4-dichlorophenylacetyl]-1-[pyrrolidin-1-yl]	C ₁₇ H ₂₄ N ₂ O	342	

Table 4. Molecular interaction data and docking energies of the molecules

Molecule Id	Hydrogen bond Interactions	Hydrophobic and Electrostatic Interactions	Docking energy (kcal.mol ⁻¹)
1	Lys55, Glu73, Glu109, Met111 and Asp169	Ile32, Val40, Ala53, Val158 and Leu168	-8.7
2	Asn114 and Ser155	Ile32, Val40 and Leu168	-5.4
3	Asn114	Ile32, Val40 Ala53, Ile86, Met108, Glu109, Leu110 Val158 and Leu168	-6.4
4	Ser34 and Asp169	Ile32, Val40 and Leu168	-8.2
5	Asp112 and Asn114	Ile32, Val40 Ala53, Ile86, Met108, Glu109, Leu110 Ala113, Val158 and Leu168	-6.3
6	Ser155 and Asp169	Gly35, Val40, Ala53 and Leu168	-5.5
7	Glu73 and Asp169	Ile32, Val40, Lys55, Val158 and Leu168	-7.9
8	Asn114	Ile32, Val40 Ala53, Lys55, Ile86, Met108, Glu109, Leu110 and Val158	-5.3
9	Asn114	Ile32, Val40 Ala53, Lys55, Ile86, Met108, Glu109, Leu110 and Val158	-5.8

interaction of oxygen of hydroxyl functionality with Ser34 in the catalytic region and the oxygen of the nitro functional group developed polar hydrogen bond contact with Asp169 in the DFG motif of the JNK-1. The bromo functional group attached on the 5th position of the naphthalene ring and ring itself established π -sigma, π - π , π -alkyl electrostatic and hydrophobic interactions with Ile32, Val40 and Leu168 with corresponding docking energy -8.2 kcal.mol⁻¹ as divulged by Figure 3B.

Compounds 3 and 7 with docking energies -6.4 and -7.9 kcal.mol⁻¹ housed in the active motif of the JNK-1 and the oxygen of the amide functionality interacted via hydrogen bond interaction with Asn114. The pyrrolidine, piperidine and the phenyl clubbed with amide functional group occupied the hydrophobic area establishing π - π and π -alkyl contacts with Ile32, Val40 Ala53, Ile86, Met108, Glu109, Leu110 Val158 and Leu168. For 7 the hydrogens of the amino group interacted via two hydrogen bonds Asp169 and Glu73 in the DFG motif and side chain region. The phenyl

ring attached with ester functional group developed π -sigma electrostatic interaction with Val40 and the octahydroquinolizine ring developed π - π and π -alkyl interactions with Ile32, Val40, Lys55, Val158 and Leu168 in the hydrophobic cavity of JNK-1 protein as stated in Figures 3C and 3D, respectively.

Molecule 2 with least docking energy -5.4 kcal.mol⁻¹ was well placed the cavity of the protein establishing two hydrogen bond interactions of the ketone carbonyl with Asn114 and Ser155. The bicyclic ring established π -alkyl hydrophobic interactions with Ile32, Val40 and Leu168 as shown in Figure 3E (Table 4).

3.4.2 Docking of Selected Compounds of *T. alata* against KAS III

Compound 4 with an excellent docking energy -8.0 kcal.mol⁻¹ encountered the active pocket of the KAS III; the oxygen of hydroxyl functionality interacted via three hydrogen bonds with Arg46 and Arg262. The phenyl and quinolone ring attached by the imine

linkage developed π -alkyl hydrophobic contacts with Arg46 and Arg223 as shown in Figure 4A.

Compound 2 was well placed in the active pocket of KAS III macromolecule establishing two hydrogen bond interactions of oxygen of ketone functionality with Asn260 and Arg262. The bicyclooctane ring developed π -alkyl hydrophobic contacts with Phe165

with corresponding docking energy of $-5.9 \text{ kcal.mol}^{-1}$ as divulged in Figure 4B (Table 5).

3.5 Antiproliferative Activities

3.5.1 Morphological Screening

A monolayer of A-549 cells got treated by $50 \mu\text{g}$ *T. coronaria* and *T. alata* and $25 \mu\text{g}$ of the standard drug

Table 5. Molecular interactions data and docking energies of the molecules

Sr. No.	Molecule Id	Hydrogen bond Interactions	Hydrophobic and Electrostatic Interactions	Docking energy (kcal.mol ⁻¹)
1	2	Asn260 and Arg262	Phe165 and Gly222	-5.9
2	4	Arg46 and Arg262	Arg46, Leu166, Met220 and Arg223	-8.0
3	6	Gly222 and Arg262	Val225	-5.6
4	8	Ala320	Val91, Ala121, Phe167, Leu196, Leu201 and Ile218	-5.4

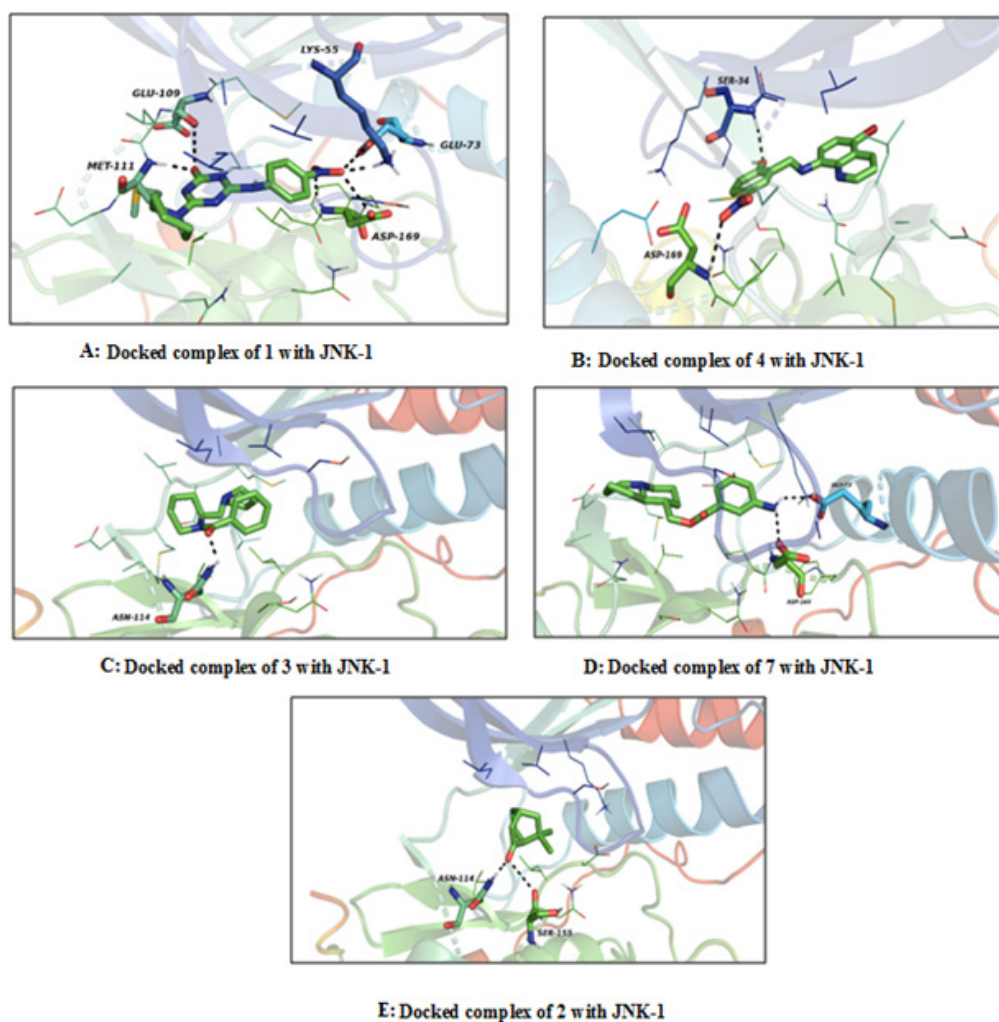


Figure 3. Various docked complexes with JNK-1.

to assess the morphological changes. Cell shape and cell volume were examined under a microscope as cell volume expansion is a crucial step in the proliferation of cells. Control cells maintained their normal cuboidal shape, 50 μ g *T. coronaria* and *T. alata* of treated

Table 6. Impact of healing group on zebra fish fin assess

Treatment Group	% Fin Regeneration
Control	76.3 \pm 0.56
Bevacizumab (250 μ g/150ml)	21.3 \pm 1.233***
<i>Tabernaemontana coronaria</i> (500 μ g/150ml)	34.0 \pm 1.599**
<i>Thunbergia alata</i> . (500 μ g/150ml)	27.3 \pm 2.014***

Cells and Bevacizumab treated cells displayed decreased cell volume expansion, altering the cell shape to a spindle shape in this assay (Figure 5).

Table 7. Impact of treatment group on zebra fish embryo test

Treatment Group	Angiogenic vessels-%
Control	95.3 \pm 1.4
Bevacizumab(25 μ g/100ml)	23.5 \pm 0.764***
<i>Tabernaemontana coronaria</i> (50 μ g/100ml)	34.0 \pm 1.60***
<i>Thunbergia alata</i> . (50 μ g/100ml)	19.0 \pm 1.36***

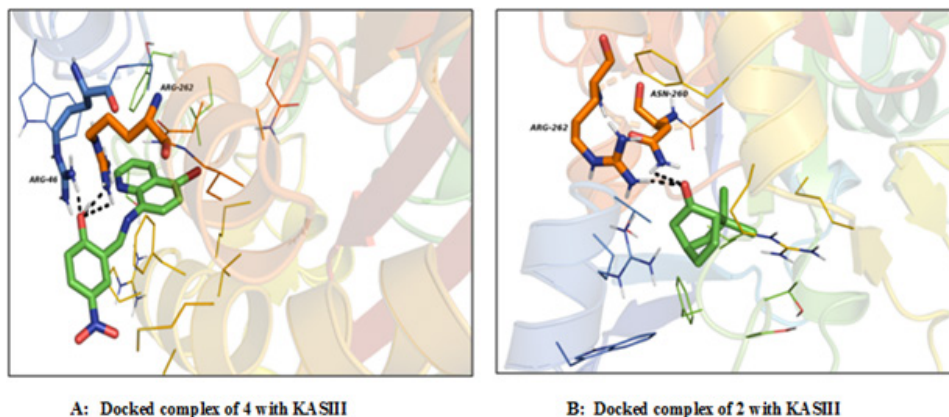


Figure 4. Various docked complexes with KAS III.

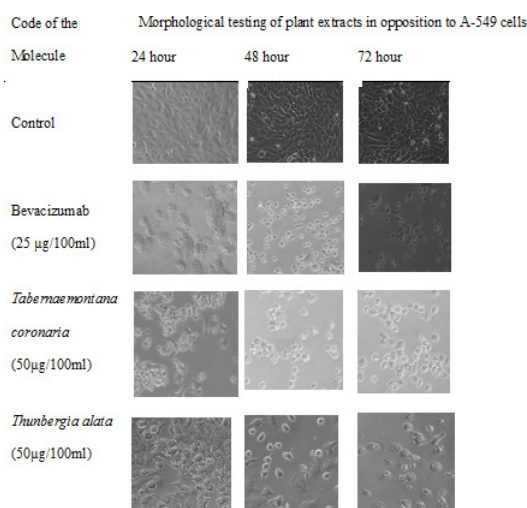


Figure 5. Morphological screening of *T. coronaria* and *T. alata* in opposition to A-549 cells.

3.5.2 Zebra Fish Fin Assay

In the regeneration of Zebra fish fin model, the mean percentage of fin regeneration estimated. The test extracts selected produced a similar standard result in Table 6, Figure 6A and Figure 7A.

3.5.3 Zebra Fish Embryo Assay

The micro blood vessels from the caudal vein and dorsal aorta, the two major blood vessels, were counted to assess the results. Intersegmental and dorsal longitudinal anastomotic vessels both developments decreased in the test and standard treatment groups. The highest dose of the test drug selected showed better result than the standard drug. All the three test doses showed significant antiangiogenic results in Table 7, Figure 6B and Figure 7B.

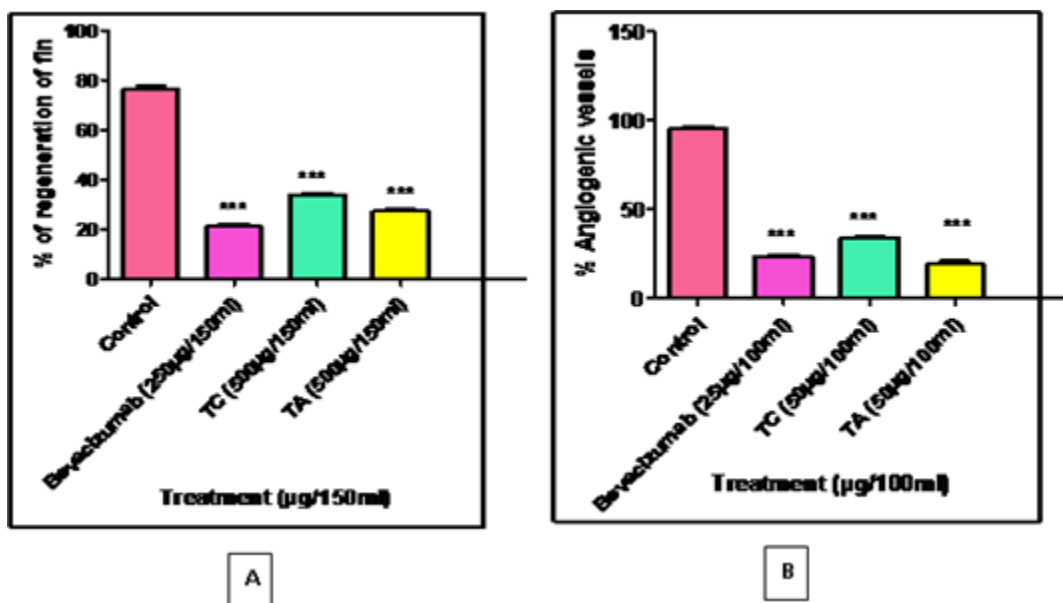


Figure 6. Graph showing the effect of plant extracts on zebra fish (A) fin assay, (B) embryo assay



Figure 7. Impact of treatment group on antiangiogenic action in (A) zebra fish embryos; (B) Renewal of zebra fish fin.

4. Conclusion

In the current study, *T. coronaria* and *T. alata* leaves have suggested different secondary metabolites which own numerous pharmacologic assets of which antioxidant property too exists. The GC-MS analysis and molecular

docking reveals the existence of bioactive constituents which result in the property like anti-inflammatory, hypercholesterolemic, anticancer, antioxidant, and antimicrobial. Henceforth, their therapeutic effects are due to the incidence of phytochemicals, which is well proven in this study. The results suggest that *T. coronaria*

and *T. alata* treatment strongly inhibited A549 cells viability, and cell volume expansion, which result in cell proliferation. Likewise, a noteworthy decrease in fin regeneration and reduction in percentage vessel growth was observed in zebra fish and embryo assays. Additional research is obligatory for development of antiproliferative molecules employing some of the bioactive components detected in the *T. coronaria* and *T. alata*.

5. Acknowledgement

SN completed the research work, execution, and writing. AM and VK did the work plan, review, and corrections. All authors agree with the submission and publication. All authors have read and agreed to the published version of the manuscript.

6. References

- Saravanan R, Raja K, Shanthi D. GC-MS analysis, Molecular docking and pharmacokinetic properties of phytocompounds from *Solanum torvum* unripe fruits and its effect on breast cancer target protein. *Appl Bio chem Bio tech nol.* 2022; 194(1):529-55. <https://doi.org/10.1007/s12010-021-03698-3> PMID:34643844 PMCID:PMC8760204
- Mahomoodally MF. Traditional medicines in Africa: An appraisal of ten potent African medicinal plants. *eCAM.* 2013; 617459. <https://doi.org/10.1155/2013/617459> PMID:24367388 PMCID:PMC3866779
- Nisha K, Darshana M, Madhu G, Bhupendra MK. GC-MS analysis and anti-microbial activity of *Psidium guajava* (leaves) grown in Malva region of India. *IJDDR.* 2011; 3(4):237-45.
- Starlin T, Prabha PS, Thayakumar BK, Gopalakrishnan VK. Screening and GC-MS profiling of ethanolic extract of *Tylophora pauciflora*. *Bio information.* 2019; 15(6):425. <https://doi.org/10.6026/97320630015425> PMID:31312080 PMCID:PMC6614127
- Kumar A, Banerjee N, Singamaneni V, Dokuparthi SK, Chakrabarti T, Mukhopadhyay S. Phytochemical investigations and evaluation of antimutagenic activity of the alcoholic extract of *Glycosmis pentaphylla* and *Tabernaemontana coronaria* by Ames test. *Nat Prod Res.* 2018; 32(5):582-7. <https://doi.org/10.1080/14786419.2017.1318384> PMID:28423921
- Ntuli SBN, Gelderblom WCA, Katerere DR. The mutagenic and antimutagenic activity of *Sutherlandia frutescens* extracts and marker compounds. *BMC Complement Altern Med.* 2018; 18(1):93. <https://doi.org/10.1186/s12906-018-2159-z> PMID:29544492 PMCID:PMC5856389
- El-Gayed SH, Kandil ZA, Abdelrahman EH. Cycloartanes from *Tabernaemontana coronaria* (Jacq) Willd flowers with their cytotoxicity against MCF7 and HCT116 cancer cell lines. *J Pharma cogn Phyto chem.* 2015; 4(3):35-41.
- Uma C, Poornima K, Surya S, Ravikumar G, Gopalakrishnan VK. Nephroprotective effect of ethanolic extract of *Tabernaemontana coronaria* in mercuric chloride induced renal damage in wistar albino rats. *Int J Chem Eng Appl.* 2012; 3(4):269. <https://doi.org/10.7763/IJCEA.2012.V3.198>
- Pushpa B, Latha KP, Vaidya VP, Shruthi A, Shweath C. *In vitro* anthelmintic activity of leaves extracts of *Tabernaemontana coronaria*. *Int J Chemtech Res.* 2011; 3(4):1788-90.
- Raghavendra HL, Prashithkekuda TR, Chetan DM. Phytochemical analysis and *In vitro* antioxidant activity of *Rubus apetalus* Poir (Rosaceae). *Pharmacol OnLine.* 2018; 1:187-95.
- Jenifer S, Priya S, Laveena DK, Singh SJ, Jeyasree J. Sensitivity patterns of some flowering plants against *Salmonella typhi* and *Pseudomonas aeruginosa*. *J Pharm Sci.* 2014; 3:1212-20.
- Housti F, Andary C, Gargadennec A, Amssa M. Effects of wounding and salicylic acid on hydroxycinnamoylmalic acids in *Thunbergia alata*. *Plant Physiol Bio Chem.* 2002; 40(9):761-9. [https://doi.org/10.1016/S0981-9428\(02\)01427-4](https://doi.org/10.1016/S0981-9428(02)01427-4)
- Damtouf S, Frederiksen LB, Jensen SR. Alatoside and thunaloside, two iridoid glucosides from *Thunbergia alata*. *Phytochem.* 1994; 35(5):1259-61. [https://doi.org/10.1016/S0031-9422\(00\)94832-5](https://doi.org/10.1016/S0031-9422(00)94832-5)
- Rady I, Bloch MB, Chamcheu RC, BanangMbeumi S, Anwar MR, Mohamed H, Babatunde AS, Kuate JR, Noubissi FK, El Sayed KA, Whitfield GK. Anticancer properties of graviola (*Annona muricata*): a comprehensive mechanistic review. *Oxid Med Cell Longev.* 2018. p. 1-39. <https://doi.org/10.1155/2018/1826170> PMID:30151067 PMCID:PMC6091294
- Ammar YA, El-Sharief AM, Belal A, Abbas SY, Mohamed YA, Mehany AB, Ragab A. Design, synthesis, antiproliferative activity, molecular docking and cell cycle analysis of some novel (morpholinylsulfonyl) isatins with potential EGFR inhibitory activity. *Eur J Med Chem.* 2018; 156:918-32. <https://doi.org/10.1016/j.ejmech.2018.06.061> PMID:30096580
- MdNesran ZN, Shafie NH, Ishak AH, MohdEsa N, Ismail A, MdTohid SF. Induction of endoplasmic reticulum stress pathway by green tea epigallocatechin-3-gallate (EGCG) in colorectal cancer cells: activation of PERK/p-eIF2 α /ATF4 and IRE1 α . *Biomed Res Int.* 2019; 2019. <https://doi.org/10.1155/2019/3480569> PMID:31930117 PMCID:PMC6942794
- Rady I, Siddiqui IA, Rady M, Mukhtar H. Melittin, a major peptide component of bee venom, and its conjugates in cancer therapy. *Cancer Lett.* 2017; 402:16-31. <https://doi.org/10.1016/j.canlet.2017.04.011>

- doi.org/10.1016/j.canlet.2017.05.010 PMID:28536009
PMCID:PMC5682937
18. Islam MR, Akash S, Rahman MM, Nowrin FT, Akter T, Shohag S, Rauf A, Aljohani ASM, Simal-Gandara J. Colon cancer and colorectal cancer: Prevention and treatment by potential natural products. *Chem Biol Interact.* 2022; 368:110170. <https://doi.org/10.1016/j.cbi.2022.110170> PMID:36202214
 19. Mahadevappa R, Kwok HF. Phytochemicals - A novel and prominent source of anti-cancer drugs against colorectal cancer. *Journal Comb Chem High Throughput Screen.* 2017; 20(5):376-94. <https://doi.org/10.2174/1386207320666170112141833> PMID:28078982
 20. Bakshi L, Ghosh R. Marigold biopesticide as an alternative to conventional chemical pesticides. *J Adv Sci Res.* 2022; 13(05):26-33. <https://doi.org/10.55218/JASR.202213503>
 21. Kumar A, Banerjee N, Singamaneni V, K Dokuparthi S, Chakrabarti T, Mukhopadhyay S. Phytochemical investigations and evaluation of antimutagenic activity of the alcoholic extract of *Glycosmis pentaphylla* and *Tabernaemontana coronaria* by Ames test. *Nat Prod Res.* 2018; 32(5):582-587. <https://doi.org/10.1080/14786419.2017.1318384> PMID:28423921
 22. Karkossa F, Klein S. Individualized *In vitro* and *in silico* methods for predicting *in vivo* performance of enteric-coated tablets containing a narrow therapeutic index drug. *Eur J Pharm Biopharm.* 2019; 135:13-24. <https://doi.org/10.1016/j.ejpb.2018.12.004> PMID:30529296
 23. Saeed N, Khan MR, Shabbir M. Antioxidant activity, total phenolic and total flavonoid contents of whole plant extracts *Torilis leptophylla* L. *BMC Complement Altern Med.* 2012; 12(1):1-2. <https://doi.org/10.1186/1472-6882-12-221> PMID:23153304 PMCID:PMC3524761
 24. Ma J, Huang J, Hua S, Zhang Y, Zhang Y, Li T, Dong L, Gao Q, Fu X. The ethnopharmacology, phytochemistry and pharmacology of *Angelica biserrata* - A review. *J Ethnopharmacol.* 2019; 231:152-69. <https://doi.org/10.1016/j.jep.2018.10.040> PMID:30408534
 25. Huang Y, Zhai Y, Huang Y, Huang Y, Liu K, Zhang J, Zhou J. Effects of light intensity on physiological characteristics and expression of genes in coumarin biosynthetic pathway of *Angelica dahurica*. *Int J Mol Sci.* 2022; 23(24):15912. <https://doi.org/10.3390/ijms232415912> PMID:36555551 PMCID:PMC9781474
 26. Sharma DK, Dave RS, Shah KR. Proximate analysis, preliminary phytochemical screening and characterization of compounds by GC-MS from "*Cycas revoluta*". *Vegetos.* 2022. p. 1-7. <https://doi.org/10.1007/s42535-021-00338-3>
 27. Wangchuk P, Keller PA, Pyne SG, Taweechotipatr M, Kamchonwongpaisan S. GC/GC-MS analysis, isolation and identification of bioactive essential oil components from the Bhutanese medicinal plant, *Pleurospermum amabile*. *Nat Prod Commun.* 2013; 8(9):1934578X1300800930. <https://doi.org/10.1177/1934578X1300800930>
 28. Aziz M, Ahmad S, Iqbal MN, Khurshid U, Saleem H, Alamri A, Anwar S, Alamri AS, Chohan TA. Phytochemical, pharmacological, and *In-silico* molecular docking studies of *Strobilanthes glutinosus* Nees: An unexplored source of bioactive compounds. *S Afr J Bot.* 2022; 147:618-27. <https://doi.org/10.1016/j.sajb.2021.07.013>
 29. Aati HY, Anwar M, Al-Qahtani J, Al-Taweel A, Khan KU, Aati S, Usman F, Ghalloo BA, Asif HM, Shirazi JH, Abbasi A. Phytochemical profiling, *In vitro* biological activities, and *in silico* studies of *Ficus vasta* Forsk.: An unexplored plant. *Antibiotics.* 2022; 11(9):1155. <https://doi.org/10.3390/antibiotics11091155> PMID:36139935 PMCID:PMC9495161
 30. Urrego D, Tomczak AP, Zahed F, Stühmer W, Pardo LA. Potassium channels in cell cycle and cell proliferation. *Philos Trans of the Royal Society B: Bio Sci.* 2014; 369(1638):20130094. <https://doi.org/10.1098/rstb.2013.0094> PMID:24493742 PMCID:PMC3917348
 31. Kamili C, Kakataparthi RS, Vattikutti UM, Chidrawar V, Ammineni S. Antiproliferative and anti-angiogenic activities of ion-channel modulators: *In ovo*, *in vitro* and *in vivo* study. *Asian Pac. J Trop Biomed.* 2017; 7(6):555-62. <https://doi.org/10.1016/j.apjtb.2017.05.005>